Direct Self-Control (DSC) of Inverter-Fed Induction Machine

M. DEPENBROCK

Abstract—**The new "direct self-control" (DSC) is a simple method of signal processing which gives converter-fed three-phase machines an excellent dynamic performance. To control the torque of, e.g., an induction motor, it is sufficient to process the measured signals of the stator currents and the total flux linkages only. Optimal performance of drive systems is accomplsihed in steady state as well as under transient conditions by combination of several two-limits controls. The expenses are less than in the case of proposed predictive control systems or flux acceleration method (FAM), if the converter's switching frequency has to be kept minimal.**

I. Introduction

IN MOST control strategies for three-phase motor drives it is assumed that the controllable power source can force any desired curves of currents or voltages into the stator windings [1], [2]. In reality most of the inverters in use can produce only seven discrete spacevector values of actuating variables. Usually none of these is exactly equal to the desired instantaneous value of the space vector. By the use of PWM the desired agreement can be obtained only for the mean values taken about a pulse period. By using high switching frequencies the desired curves of actuating variables can be approximated sufficiently well. However, in the field of high power applications this is not possible; for economic reasons the switching frequencies of high-power semiconductors can't be raised above values of 200–300 Hz. Therefore it is desirable to derive the single switching commands directly from suitable control signals as, e.g., according to predictive current control [3] or improved flux acceleration method (FAM) [4].

This paper describes a recently developed direct self-control (DSC) method [5]–[7]. By consistent adoption of the strategies to guide the stator flux and to control the torque according to the switching capabilities of voltage source inverters (VSIs) we get not only very simple and robust signal processing schemes but also excellent dynamic performance even at the low switching frequencies used in the high-power electronics field.

Manuscript received November 11, 1987; revised July 12, 1988. This paper is a revised version of a work presented at the IEEE Power Electronics Specialists Conference, Blacksburg, VA, June 16–21, 1987.

The author is with Ruhr-University Bochum, 463 Bochum 1, Universitätsstrasse 150, Gebäude IC-FO-04/560, West Germany.

IEEE Log Number 8823455.

II. Basic Circuit and Steady-State Performance of Inverter-Fed Three-Phase Machines with DSC

The shaft speed of a three-phase machine mainly depends on the angular velocity of the rotating magnetic field. In steady state this velocity is determined by the frequency f_s of electric stator quantities; the magnitude of the magnetic field depends on the voltage to frequency ratio. Fig. 1 shows how the on–off states of the power switching elements of a three-phase VSI can be directly controlled by comparing the time integrals of its own line-to-line voltages to reference values $\pm\Psi_{\text{ref}}$. This is called "direct self-control" (DSC) for the sake of brevity. In doing so the magnitude of the magnetic field is directly determined by Ψ_{ref}. Without pulse control the frequency depends on the ratio of dc voltage $2E_d$ to Ψ_{ref}. For further simplification the time integral of a voltage will now always be called "flux," regardless of whether the voltage is caused by variation of a flux linkage or not.

Fig. 2 shows the curves of line-to-line voltage $e_{bc} = \sqrt{3}\, e_{\beta a}$ of all processed fluxes $\Psi_{\beta\nu}$ ($\nu = a; b; c$), of all line-to-dc-center point voltages $e_{\nu C}$, and of line-to-neutral voltage $e_{ao} = e_{\alpha a}$. The β-fluxes are proportional to the time integrals of line-to-line voltages; α-signals correspond to line-to-neutral quantities. From Fig. 2 it can be seen that the following equations hold in steady state:

$$\hat{\Psi}_\beta - \check{\Psi}_\beta = 2\Psi_{\text{ref}} = 2E_d/\sqrt{3} \cdot T_s/3$$

$$f_s = \frac{1}{6} \cdot \frac{2E_d/\sqrt{3}}{\Psi_{\text{ref}}} \tag{1}$$

$$\hat{\Psi}_f = 2/\sqrt{3} \cdot 9/\pi^2 \cdot \Psi_{\text{ref}} = 1,05 \cdot \Psi_{\text{ref}}. \tag{2}$$

The curves show that the deviations of the real fluxes $\Psi_{\beta\nu}$ from their fundamental components $\Psi_{f\nu}$ are so small that the three-phase machine with DSC in steady state will have nearly the same performance as one being line supplied by sinusoidal voltages. In order to get nominal flux, $\hat{\Psi}_{f0}$, the corresponding value of Ψ_{ref} can be derived from (2). The speed of shaft rotation can be controlled by variation of the dc voltage $2E_d$ according to (1). To raise the speed above the highest possible value at full dc voltage and full flux the magnitude of flux can be weakened by decreasing Ψ_{ref}. If all terminals of the machine are connected simultaneously to one of the two dc terminals by

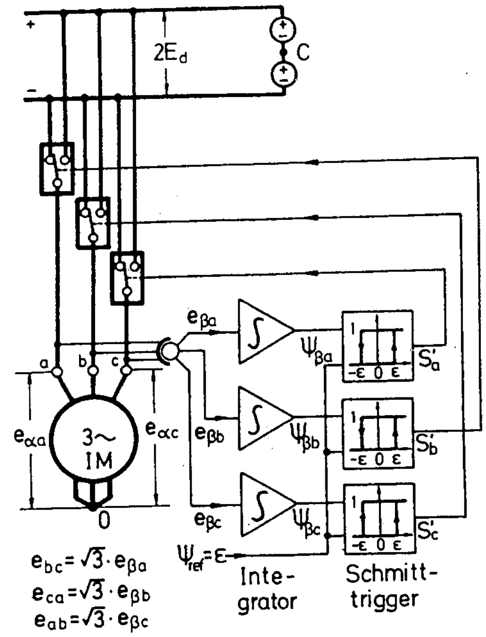

Fig. 1. Basic scheme of DSC.

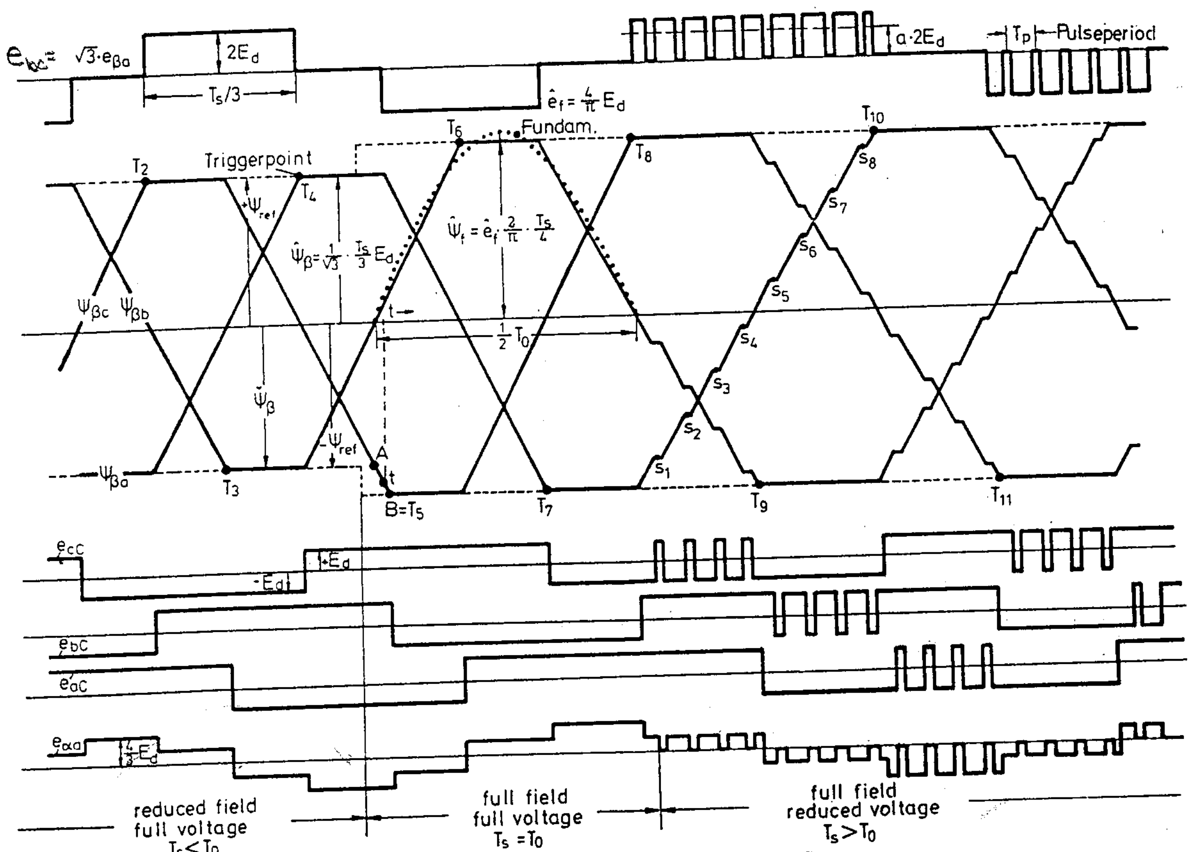

Fig. 2. Curves of stator quantities with DSC.

the inverter, all terminal voltages of the machine will be zero. This can be done in addition to the normal switchings caused by the Schmitt triggers via a single modulating device, as described later. In this way, instead of controlling $2E_d$, the terminal voltages of the three-phase machine can be reduced by PWM as shown in the right portion of Fig. 2. If the pulse period T_p is short relative to the smallest time constant of the machine, a very simple feed-forward control is possible.

The dynamic properties of DSC can be represented by the response to a step change of motor voltage, via $2E_d$ or by pulse control, keeping Ψ_{ref} constant, or vice versa. To illustrate the theory the induction machine is chosen as an example.

III. Response of Rotor Quantities of an Induction Machine on Step Change of Slip

Fig. 3 shows the track curve of space vector $\vec{\Psi}_s$, which we get by transforming the three β_ν-flux quantities of Fig. 2 into a space-vector representation by the formula

$$\vec{\Psi}_s = j\tfrac{2}{3}[\Psi_{\beta a} + a\Psi_{\beta b} + a^2\Psi_{\beta c}]$$

$$= \tfrac{2}{3}[\Psi_{\alpha a} + a\Psi_{\alpha b} + a^2\Psi_{\alpha c}]$$

$$a = \exp(2\pi/3) \quad (3)$$

Usually the lower representation is taken, if the line-to-neutral voltages are chosen as input quantities, of which the time integrals are forming the α_ν-fluxes. At constant dc voltage $2E_d$ the space vector $\vec{e}_s$ of VSI output voltages can assume only seven discrete values, characterized in Fig. 3 by the points $0 \cdots 6$. According to

$$\dot{\vec{\Psi}}_s = \vec{e}_s, \quad (4)$$

$|\vec{e}_s|$ determines the tracking speed with which the head of $\vec{\Psi}_s$ traverses its track curve. That means tracking speed depends only on the instantaneous value of $2E_d$, if we don't have just a stop of motion, when zero value $\vec{e}_s(0)$ is realized during a part of the pulse period. The direction of $\vec{e}_s$ gives the direction of the straight lines forming the track curve of $\vec{\Psi}_s$. With DSC the distance of the straight parts of the track curve from the tail of $\vec{\Psi}_s$ is given by Ψ_{ref}. The projections of the moving $\vec{\Psi}_s$ on the three β_ν-axes give the curves of the β_ν-fluxes, which are compared to $\pm\Psi_{ref}$. Keeping Ψ_{ref} constant, the track curve of $\vec{\Psi}_s$ forms a regular hexagon. Its center point is lying on the origin of the complex plane, independent of preceding changes of Ψ_{ref}. At constant dc voltage and without pulse control, the track speed of $\vec{\Psi}_s$ remains constant, and magnitude and angular speed of this space vector are slightly pulsating. The points of Fig. 3 identified by capital letters correspond to the points with those letters in Fig. 2.

The question about the dynamic properties of the induction machine with DSC can be divided into two problems, first the response to a step change of track speed keeping the track curve unchanged and second the response to variation of the track curve by a stepwise change of Ψ_{ref}, keeping the track speed constant. The form of solutions should be as obvious as possible and be based on the well-known steady-state representation of the induction machine. To change the track speed of space vector $\vec{\Psi}_s$ chiefly means to vary the instantaneous slip of magnetic field relative to the rotor conductors of the induction machine. All consequences concerning torque and currents depend only on slip and not on shaft speed. Only stator voltages depend on the angular speed ω of the shaft.

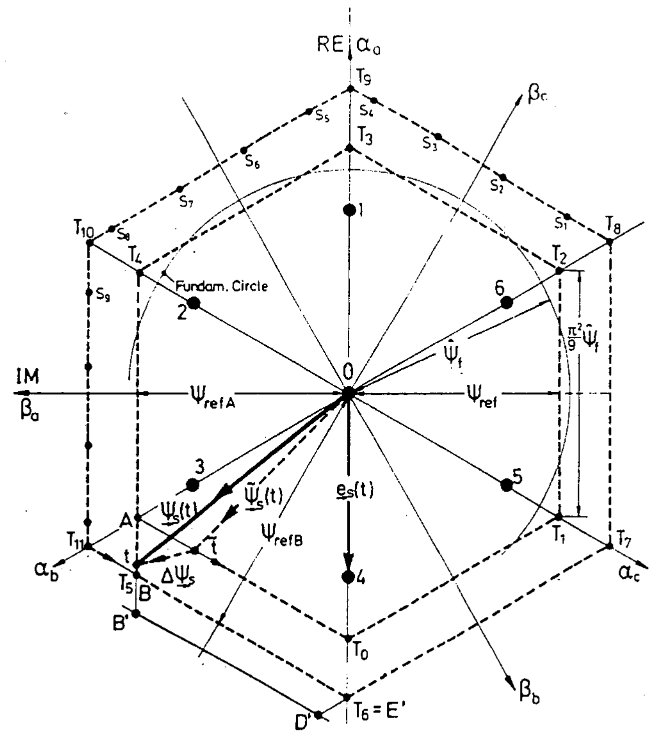

Fig. 3. Space vectors of stator voltages, total fluxes, and track curves with DSC.

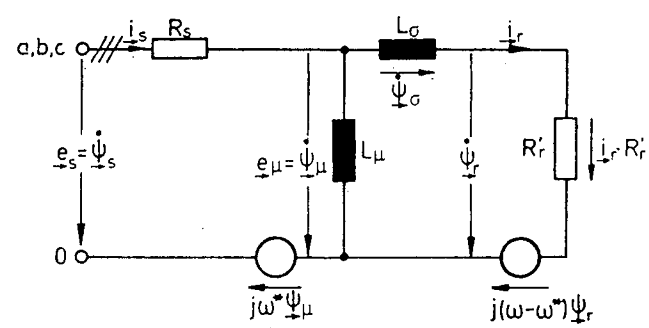

Fig. 4. Equivalent circuit and space vector quantities of ideal induction machine with two poles at angular speed ω.

Therefore, if we want to describe the response to a step change of slip, it is most reasonable to choose a reference frame fixed to the rotor. Fig. 4 shows an exact equivalent circuit of the fundamental wave three-phase induction machine with one pair of poles, and without skin effect.

ω^* means the angular speed of used reference frame relative to the stator. In the chosen case of rotor fixed frame, ω^* is equal to the angular speed ω of the shaft. Because of $j(\omega - \omega^*) \cdot \vec{\Psi}_r \equiv 0$ there is no influence of any rotor phase upon each other. Concerning the space vector of fluxes, currents, and resultant voltages, their magnitudes and angular displacements do not depend on ω^*, only the derivations of the latter do. As noted before, if we keep Ψ_{ref} constant, we may approximate without essential error the hexagonal track curve of $\vec{\Psi}_s$ by the circle (see Fig. 3) corresponding to the fundamental components of total fluxes in steady state. Then we may express the space vector $\vec{\Psi}_{\mu f}$, which rotates counterclockwise with angular speed ω_r relative to three projection lines α_a', α_b', α_c', by

$$\vec{\Psi}_{\mu f} = -j \cdot \hat{\Psi}_{\mu f} \cdot e^{j\omega_r t}. \tag{5}$$

With magnitude $\hat{\Psi}_{\mu f}$ being constant we get the space vector $\vec{e}_\mu$ of voltages across the three series connections of L_σ and R_r' from

$$\vec{e}_\mu = \dot{\vec{\Psi}}_{\mu f} = j\omega_r \cdot \vec{\Psi}_{\mu f} = \omega_r \cdot \hat{\Psi}_{\mu f} \cdot e^{j\omega_r t}$$

$$\hat{e}_0 = \omega_0 \cdot \hat{\Psi}_{f0} \quad \text{(nominal values)}. \tag{6}$$

We get all line-to-neutral values of rotor quantities by projection of the corresponding space vectors on the projection lines α_a', α_b', α_c'. Under sinusoidal conditions at constant angular slip frequency ω_r, the track curves relative to the projection lines of all space vectors are circles, which are traversed counterclockwise with identical angular speed ω_r. If we rotate the projection lines clockwise with angular speed ω_r in the complex plane, all space vectors assume fixed positions; we get the well-known phasor representation of induction machine quantities. If the angular frequency ω_r is varied, the Heyland circle shown in Fig. 5 is obtained, which is the locus curve of the space vectors $\vec{i}_s$, $\vec{i}_r = \vec{\Psi}_\sigma/L_\sigma$, and $\vec{\Psi}_r/L_\sigma = (\vec{\Psi}_\mu - \vec{\Psi}_\sigma)/L_\sigma$. The rotor fluxes $\Psi_{r\nu}$ can be explained as the time integrals of voltages $i_{r\nu} \cdot R_r'$, similar to $\Psi_{\sigma\nu}$ being the time integrals of voltages $L_\sigma \cdot i_{r\nu}$. From the flux angle ϑ we get the relative rotor frequency n_r by

$$n_r = \omega_r/\omega_K = \tan \vartheta, \quad \omega_K = R_r'/L_\sigma = 1/T_\sigma, \tag{7}$$

ω_K being the angular rotor frequency at breakdown point K. The space vectors of the stator and rotor currents only lie on the circular locus curve shown in Fig. 5 during steady-state operation with a constant magnitude $|\vec{\Psi}_\mu|$ of the resulting flux and at constant angular rotor frequency ω_r. Every other point of the current space vector plane corresponds to values of the two linearly independent state quantities of the three rotor currents, which are in principle also possible under dynamic conditions. If we, e.g., choose a value of the space vector $\vec{e}_r$ according to (6) with a value ω_{rP} of the rotor frequency, which results in steady-state operation in the rotor currents determined by the point P on the current locus curve, then the transition into the associated periodic operating condition can be readily described from any starting condition at $t = 0$. The starting state for $t = 0$ is characterized in Fig. 5 by point S. At this point in time the differences between the instantaneous rotor curents and the rotor currents, which would flow under stationary conditions at this point in time, are represented by their space vector $\vec{i}_{PS}(0)$. The projections of this space vector onto the rotating axes α_a', α_b', α_c' at time $t = 0$ furnish the starting values of the transient components of the currents. All three of them decay to zero with the same time constant $T_\sigma = L_\sigma/R_r'$. Considered relative to the rotating axes, the space vector $\vec{i}_{PS}(t)$ retains its direction, since all three transient components of rotor currents change so uniformly that their ratios remain unchanged. Only the magnitude $|\vec{i}_{PS}(t)|$ is decreasing with

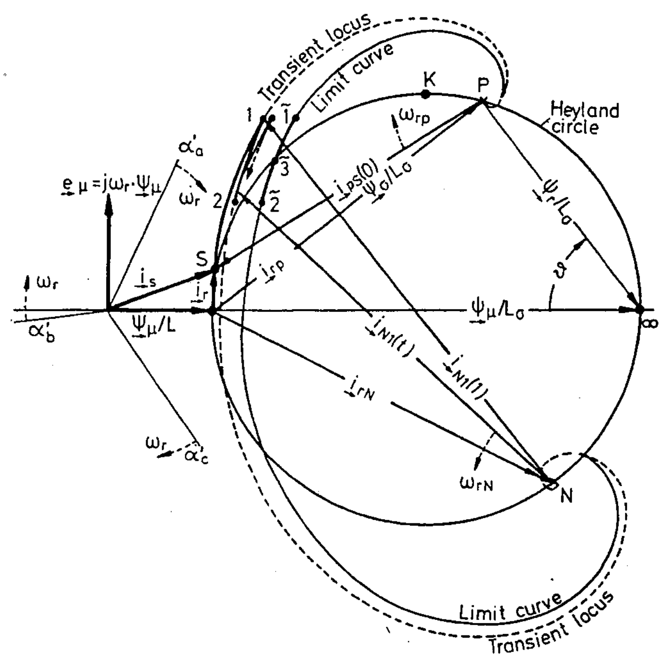

Fig. 5. Steady-state and transient locus curves of space vector quantities of induction machine.

the time constant T_σ. If the transient space vector $\vec{i}_{PS}(t)$ is considered relative to the locus curve circle, which is stationary in Fig. 5, a space vector rotating clockwise with the constant angular velocity ω_{rP} is obtained with a magnitude which is decaying to zero with the time constant T_σ. The track curve of the transient space vector $\vec{i}_{PS}(t)$ is therefore a spiral, of which the convergence center is at point P.

As shown in Fig. 5, the component of $\vec{i}_r(t)$, which is orthogonal to $\vec{\Psi}_\mu$, and therefore the torque of the machine, grows very fast after $t = 0$ because $\omega_{rP} > \omega_K$. If the stator voltage is changed, e.g., to zero upon reaching point 1 on the dynamic track curve the angular rotor frequency shall assume the large negative value ω_{rN}. The stationary point N on the locus curve circle is associated with this new angular rotor frequency. This point is now the center of convergence of the new dynamic space vector $\vec{i}_{N1}(t)$, of which the magnitude also decreases exponentially with the time constant T_σ. However, the space vector $\vec{i}_{N1}(t)$ rotates counterclockwise with the angular velocity $|\omega_{rN}|$, because the projection axes α_a', α_b', α_c' now also rotate in this sense. As may be seen directly, the torque of the machine now decreases very quickly. If the angular rotor frequency is again made equal to ω_{rP} at point 2 of the new dynamic track spiral, the initially described processes are repeated with somewhat larger overall values of that component of the rotor current space vector $\vec{i}_r$ lying in the direction of $\vec{\Psi}_\mu$. If the method of switching between the angular rotor frequencies ω_{rP} and ω_{rN} is continued in the manner described above each time the same upper or lower torque value is reached, a stationary limit cycle with the limit transient track curves shown in Fig. 5 is obtained. The starting and ending points of the cyclically traversed sections of both transient track spirals coincide and are designated in Fig. 5 by symbols $\tilde{1}$ and $\tilde{2}$. The sections of the two transient locus curves located between these two points are so close together that no difference can be noted in Fig. 5. Point $\tilde{3}$ is associated with the fundamentals of the three rotor currents, and it lies on the circular locus curve.

An infinite number of transient spirals lead to each center of convergence P of the Heyland circle. If we choose a starting point S lying on the Heyland circle at a step change of slip ($t = 0$), then, e.g., the flux-angle ϑ_S is a suitable parameter to differ between all spirals leading to P. If we refer fluxes to nominal value $\hat{\Psi}_{f0}$ and currents to $\hat{\Psi}_{f0}/L_\sigma$, we get the per-unit (pu) quantities $\psi \cdots$ and $y \cdots$. Considering the transient space vector $\vec{\Psi}_{PS}$ with its tail fixed to point P, and its head passing point S at $t = 0$, we get the equations

$$\vec{\psi}_{PS} = \vec{y}_{PS} = \vec{y}_{PS}(0) \cdot \exp(-t/T_\sigma) \cdot \exp(-j\omega_{rP}t)$$

$$\vec{y}_{PS}(0) = \sin\vartheta_S \cdot \exp(-j\vartheta_S) - \sin\vartheta_P \exp(-j\vartheta_P)$$

$$= \sin(\vartheta_S - \vartheta_P) \cdot \exp[-j(\vartheta_S + \vartheta_P)]. \quad (8)$$

When $\vec{\Psi}_{PS}$ crosses the Heyland circle in point S, the direction of the transient track curve is equal to the direction of $\vec{\Psi}_{\sigma S}$; this means the magnitude of space vector $\vec{\Psi}_r(t \approx 0)$ keeps unchanged near point S. Angular speed of $\vec{\Psi}_r(t \approx 0)$ relative to space vector $\vec{\Psi}_\mu$ of total fluxes is, at this point,

$$\dot{\vartheta}(t \approx 0) = \Delta\omega_{rS} = \omega_{rP} - \omega_{rS}. \quad (9)$$

Based on this understanding of response to step change of slip, for simplicity results have been derived in the rotor fixed reference frame, a very simple direct two-limit control of torque can be established and this in the stator fixed frame ($\omega^* = 0$) to avoid the coordinate transformations usually needed in field-oriented controls.

IV. Direct Two-Limit Control of Torque

Fig. 6 shows the basic circuit of a direct two-limit control of torque and of superimposed speed control. The electromagnetic torque T_q of a rotating field machine can be calculated by the following relation, all quantities corresponding to the stator fixed reference frame ($\omega^* \equiv 0$):

$$T_q = 1,5(\Psi_{\alpha a} \cdot i_{\beta a} - \Psi_{\beta a} \cdot i_{\alpha a}). \quad (10)$$

In the expanded signal processing structure shown in Fig. 6 this quantity, calculated by the torque computing unit TC, is compared with the torque reference value T_{ref} in the Schmitt trigger ST_T. Within the full-flux speed range a simple control works as follows: If the torque T_q exceeds its reference value by more than chosen tolerance value ϵ_T, then zero voltages are switched on to the motor as long as the torque T_q underpasses T_{ref} by more than ϵ_T. If this happens, full voltage is switched on to the machine, the direction of the corresponding space vector is determined by the fluxes-comparing Schmitt triggers ST_Ψ, as shown in detail before. In this state the electronic signal select ESS connects the output signals S_a', S_b', S_c' of Schmitt triggers ST_Ψ directly to the control outputs S_a, S_b, S_c as symbolically shown in Fig. 6. When zero voltages have to be switched on to the machine, a common signal S_z is connected simultaneously to all three control outputs by means of the ESS. The two possible values of S_z are chosen by the zero select unit ZS such that secondary conditions can be met, concerning, e.g., minimum switching frequency, allowed minimum duration of switching states, etc.

At lower values of stator frequency f_s the difference between $\vec{\Psi}_s$ and the space vector of total flux linkages $\vec{\Psi}_\mu$ cannot be neglected, since $|\vec{e}_\mu|$ decreases proportional to f_s and therefore $|\vec{i}_s \cdot R_s|$ gets more and more influence. Because $|\vec{\Psi}_\mu|$ should be kept, as far as possible, independent of f_s or $\vec{i}_s$ in the expanded signal processing structure shown by Fig. 6, the quantity $(\vec{e}_s - \vec{i}_s R_s) = \vec{e}_\mu$ is integrated to get the needed signals $\Psi_{\alpha a}$ and $\Psi_{\beta a}$. By means of simple algebraic calculations from these quantities the two additional needed input signals $\Psi_{\beta b}$ and $\Psi_{\beta c}$ of Schmitt triggers ST_Ψ are determined by the coordinate transformation unit CT. This kind of signal processing works sufficiently well down to values of frequency f_s near to the nominal value of the slip frequency. Fig. 7 is taken from a CRT display showing the track curve of space vector $\vec{\Psi}_\mu$ at zero r/min of shaft ($\omega = 0$) and at about nominal value of torque (inner trace) in comparison to the track curve measured at about half nominal speed. By self-control under load conditions the track curve turns relative to the no-load curve as far as the voltages of the inverter get the needed components orthogonal to the track curve to cancel the decreasing influence of $\vec{i}_s \cdot R_s$ on the magnitude of flux. If the drive is to work under conditions which lead to values of stator frequencies clearly below the nominal value of slip frequency, additional control of $|\vec{\Psi}_\mu|$ has to be provided [6], and instead of integration of induced voltages, other known methods have to be applied to determine total flux linkages. The measured response of torque of a 66 kW motor due to large and small step changes of its reference value is given later in Fig. 9(a).

At low speeds of shaft, such as in the range below 30 percent of the highest speed at full field, the dynamic performance can be further improved in the case of large control error ΔT_q caused by suddenly decreasing reference value T_{ref}. In this case, instead of the space vector of voltages having zero magnitude, the space vector $\vec{e}_s = -1 \cdot \vec{e}_s'$ can be switched on, $\vec{e}_s'$ being the space vector selected by the Schmitt triggers at counterclockwise movement of $\vec{\Psi}_\mu$. Now the space vector $\vec{\Psi}_\mu$ not only stops but it moves along the track curve, which it previously traversed counterclockwise, with full speed in the opposite direction. By this, even at very low speed of shaft, large negative values of angular rotor frequency ω_r can be achieved, which are necessary if the torque is to be decreased very fast. If the demands concerning steady state and dynamic quality of speed control are moderate, a very simple signal processing without equipment for direct measuring of shaft speed is possible, as shown in Fig. 6. At constant dc voltage the averaged output voltage of Schmitt trigger ST_T is proportional to mean value $\bar{\omega}_s$ of the angular stator frequency. By means of algebraic calculations from the torque reference value the correspond-

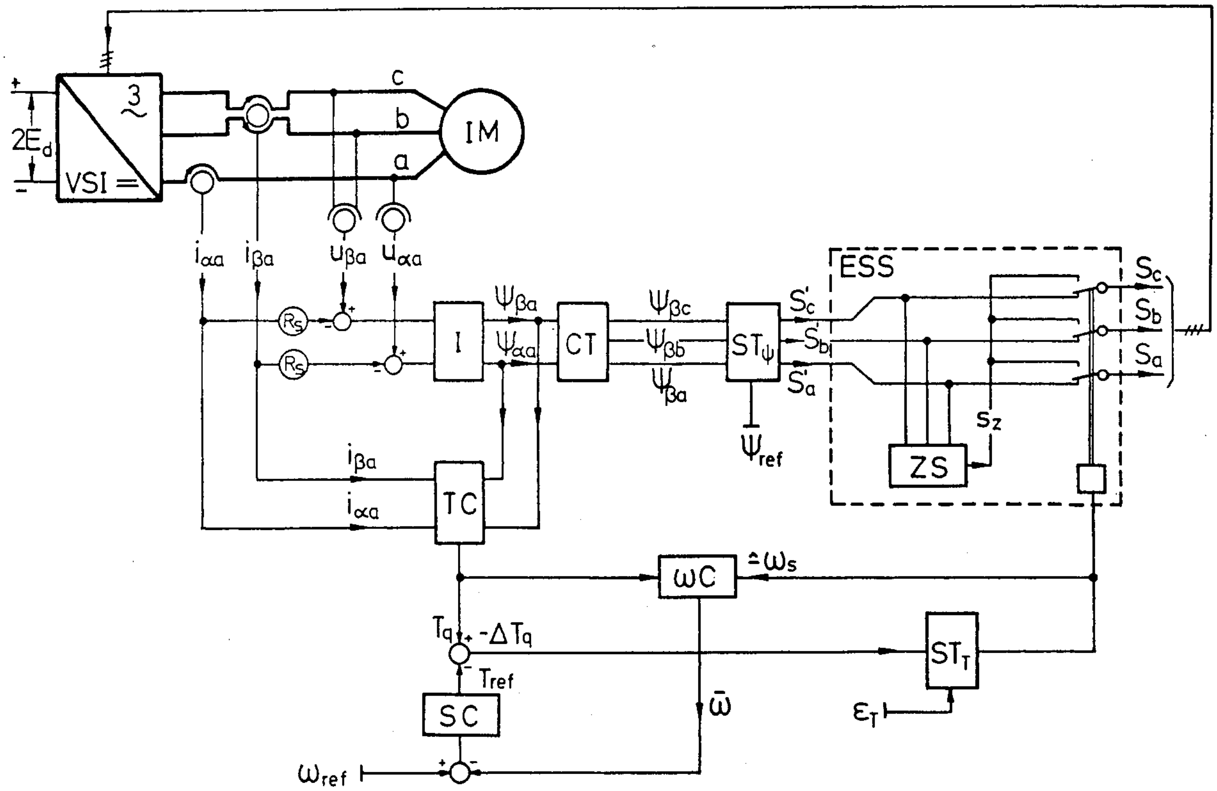

Fig. 6. Extended scheme of signal processing with DSC.

I	Integrator	ZS	Zero State Select
ST	Schmitt Trigger	TC	Torque Calculator
CT	Coordinate Transformation	ωC	Speed Calculator
ESS	Electronic Signal Select	SC	Speed Controller

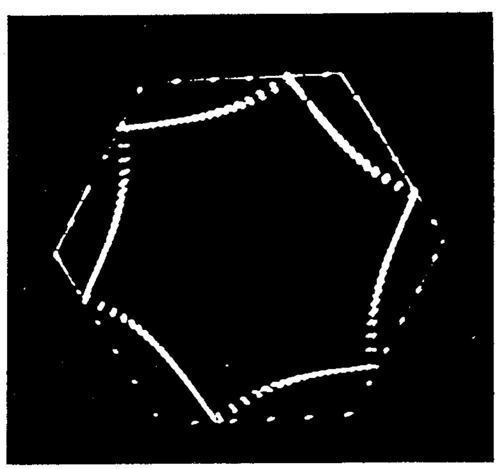

Fig. 7. Track curves of space vector $\vec{\Psi}_\mu$. Inner trace: $\omega = 0$, $T_q \approx T_{qK}/2$. Outer trace: $\omega \approx \omega_0/2$, $T_q = 0$.

ing mean value $\overline{\omega}_r$ of the angular rotor frequency can be determined. $\overline{\omega}_s - \overline{\omega}_r = \overline{\omega}$ is the quantity to be compared to reference value ω_{ref}. The output of speed controller SC gives the torque reference value T_{ref}.

V. Torque Response in the Field Weakening Range

If the inverter produces its highest possible output voltages, there are only the values $1 \cdots 6$ of $\vec{e}_s$, which have to be switched on in cyclic sequence. By this kind of operation, called fundamental frequency switching, we cannot fulfill the condition of (5) and (6). $|\Psi_\mu|$ to be constant. To investigate the dynamic behaviour of an induction machine fed by VSI in the field weakening range, therefore, the limited switching capabilities have to be fully accounted for. Furthermore, the errors caused by assuming $R_s = 0$ remain negligible; therefore we can note $\vec{\Psi}_s = \vec{\Psi}_\mu = \vec{\Psi}$. Fig. 3 shows what happens after a step change of Ψ_{ref}. After point A there is a difference $\Delta\vec{\Psi}$ between the actual space vector of fluxes $\vec{\Psi}$ and $\vec{\hat{\Psi}}$, increasing linearly with time, which is the value of the space vector of fluxes we would have got at the same point in time if we had had no change of Ψ_{ref}. $\Delta\vec{\Psi}$ does not change its direction until point B, where all total fluxes are in new steady state. Space vector $\Delta\vec{\Psi}_r$ is the response of $\vec{\Psi}_r$ due to ramp change $\Delta\vec{\Psi}$ of $\vec{\Psi}$. At point B we get

$$\left.\begin{aligned} \Delta\vec{\Psi}_{rB} &= \Delta\vec{\hat{\Psi}} \cdot \frac{\exp\left(p_r \Delta t_B - 1\right)}{p_r T_\sigma \cdot \left(p_r \Delta t_B - 1\right)} \\ \left|\Delta\vec{\hat{\Psi}}\right| &= \frac{2}{\sqrt{3}} \cdot \left[\Psi_{\text{ref}A} - \Psi_{\text{ref}B}\right] \\ \Delta t_B &= t_B - t_A \end{aligned}\right\} . \quad (11)$$

p_r is one of the two complex eigenvalues of the induction machine. Under the assumption $R_s = 0$ we get

$$p_s T_\sigma = 0 \quad p_r T_\sigma = -1 + jn \quad n = \omega/\omega_K. \quad (12)$$

If we only change from one steady-state track curve to a new one as shown by Fig. 3, after $t = t_B$, $\vec{\Psi}$ is again in steady state. $\vec{\Psi}_{rB} = \vec{\hat{\Psi}}_{rB} + \Delta\vec{\Psi}_{rB}$ being an exact known

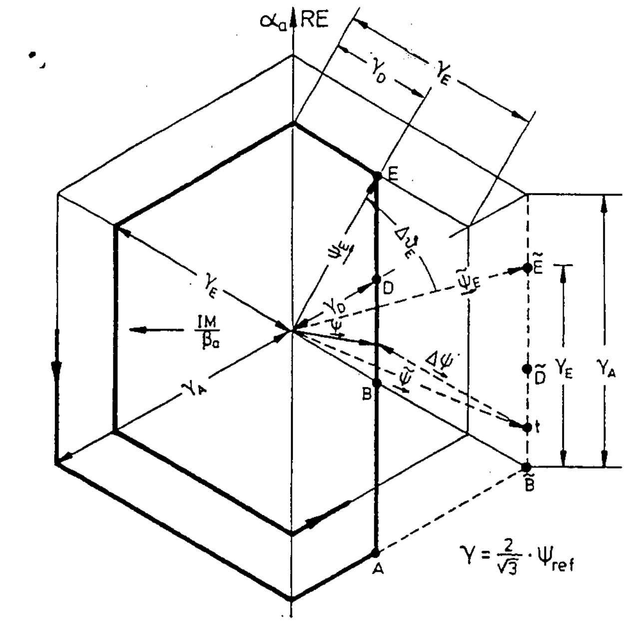

Fig. 8. Track curve of space vector $\vec{\Psi}$ at fast rise of torque by transient field weakening.

quantity, without essential error the following response of rotor quantities can be treated like the response of slip to step change, according to the results of the last chapter, because both $|\vec{\Psi}_\mu|$ and ω_r remain practically constant after point B. Because $\Delta\omega_r$ normally remains smaller than ω_K, the speed of torque change is rather low [7]. Fig. 8 shows which track curve of $\vec{\Psi}$ has to be chosen if the torque has to be changed, e.g., from no load to breakdown value, as fast as possible, shaft speed having nominal value ω_0, and this angular speed is assumed to be nine times ω_K. From point A to point B $\Delta\vec{\Psi}$ is increasing proportional to time, from point B to point E $\Delta\vec{\Psi}$ remains constant. During the last interval response $\Delta\vec{\Psi}_r$ of $\vec{\Psi}_r$ can be easily calculated as response on step change $\Delta\vec{\Psi}$ of $\vec{\Psi}$. Under the assumption $R_s = 0$ the final value of $\Delta\vec{\Psi}_r$ at $t = t_E$ is

$$\left.\begin{aligned} \Delta\vec{\Psi}_{rE} &= \Delta\hat{\vec{\Psi}}\,\frac{[\exp(p_r\Delta t_B) - 1][\exp(p_r\Delta t_E)]}{p_r T_\sigma \cdot (p_r\Delta t_B - 1)} \\ |\Delta\hat{\vec{\Psi}}| &= \frac{2}{\sqrt{3}}[\Psi_{refA} - \Psi_{refD}]; \\ \Delta t_B &= t_B - t_A;\ \Delta t_E = t_E - t_B \end{aligned}\right\} . \quad (13)$$

After point E, $\vec{\Psi}$ is again in steady state. If we demand that the mean value of torque assumes at $t = t_E$ a set value $\overline{T}_{qE}$, it is reasonable to express the mean value of torque by that component of torque T_{qf} generated by the fundamental component of $\vec{\Psi}$ and $\vec{\Psi}_r$ at $t = t_E$:

$$\left.\begin{aligned} T_{qfE} &= \frac{3}{2L_\sigma}\,\hat{\Psi}_{fE} \cdot |\vec{\Psi}_{rE}| \cdot \sin\vartheta_{fE} = \overline{T}_{qE} \\ \hat{\Psi}_{fE} &= \frac{9}{\pi^2} \cdot \frac{2}{\sqrt{3}}\,\Psi_{refE}; \\ &\vartheta_f \text{ angle between } \vec{\Psi}_f \text{ and } \vec{\Psi}_r \end{aligned}\right\} . \quad (14)$$

To get value $\overline{T}_{qE}$ at $t = t_E$ the corresponding Ψ_{refD} can be calculated from (13) and (14) and the equation of angle between $\vec{\Psi}$ and $\vec{\Psi}_f$, well-known in the case of steady-state fundamental switching. In the case of our example, under the conditions mentioned above, we get

$$\Psi_{refA} = \Psi_{ref0};\ \Psi_{refE} = 0.9\Psi_{ref0};\ \Psi_{refD} = 0.5458 \cdot \Psi_{ref0}.$$

Fig. 9(b) shows the results of a corresponding computer simulation. To decrease torque under fundamental frequency switching conditions as fast as possible we have to realize $\Psi_{refD} > \Psi_{refE} > \Psi_{refA}$, e.g., by taking a transient track curve as shown in Fig. 3, leading from point A via B' and D' to E'. In this case $\Delta\vec{\Psi}_r$ can be calculated also by combinations of ramp response and step response but the relation corresponding to (13) is somewhat more complicated. Fig. 9(c) shows the results obtained by a simple suboptimal torque control for a 50-kW drive under fundamental frequency switching conditions.

VI. Consideration of Distortion Quantities in Heyland Diagram

In steady state, deviation between rotor fluxes $\Psi_{r\nu}$ and their fundamental components can be neglected without remarkable error. That means that in the stator fixed reference frame the space vector $\vec{\Psi}_r = \vec{\Psi}_{rf}$ traverses, relative to projection axes α_a, α_b, α_c, a circular track curve with constant angular speed $\overline{\omega}_{sf}$, as shown in Fig. 10. If the same is assumed of space vector $\vec{\Psi}_{\mu f}$, representing fundamentals of $\Psi_{\mu\nu}$, the projections of space vector $\vec{\Psi}_{\sigma f} = \vec{\Psi}_{\mu f} - \vec{\Psi}_r$ give those components of leakage fluxes, connected by L_σ to fundamentals of rotor currents. The space vector of distortion fluxes due to the noncircular shape of track curve

$$\vec{\Psi}_h = \vec{\Psi}_\mu - \vec{\Psi}_{\mu f} \quad (15)$$

forms a connection between the circular track curve of $\vec{\Psi}_{\mu f}$ and the distorted track curve of $\vec{\Psi}_\mu$, represented by dotted lines in Fig. 10. In the case of direct two-point control of torque its mean value remains practically constant in steady state. Theoretically the alternating portion of torque can be made indefinitely small by increasing pulse frequency. All quantities in the limit case $T_p = 0$ give fair approximations of their mean values at $T_p > 0$. Therefore quantities of thought limit case $T_p = 0$ shall be expressed by mean value variables with overbars. Then the tracking speed of $\overline{\vec{\Psi}}_\mu$ is adjusted automatically by the torque control such that there is no difference between the directions of distortion space vector $\overline{\vec{\Psi}}_h$ and rotor fluxes representing space vector $\vec{\Psi}_r$, because only then the distortion fluxes do not disturb the constant torque generated by fundamental quantities.

If we now rotate the projection axes α_a, α_b, α_c clockwise with angular speed $\overline{\omega}_{sf}$, then all fundamental quantities keep fixed positions in the complex plane and we get the Heyland diagram shown in Fig. 11. If we add the

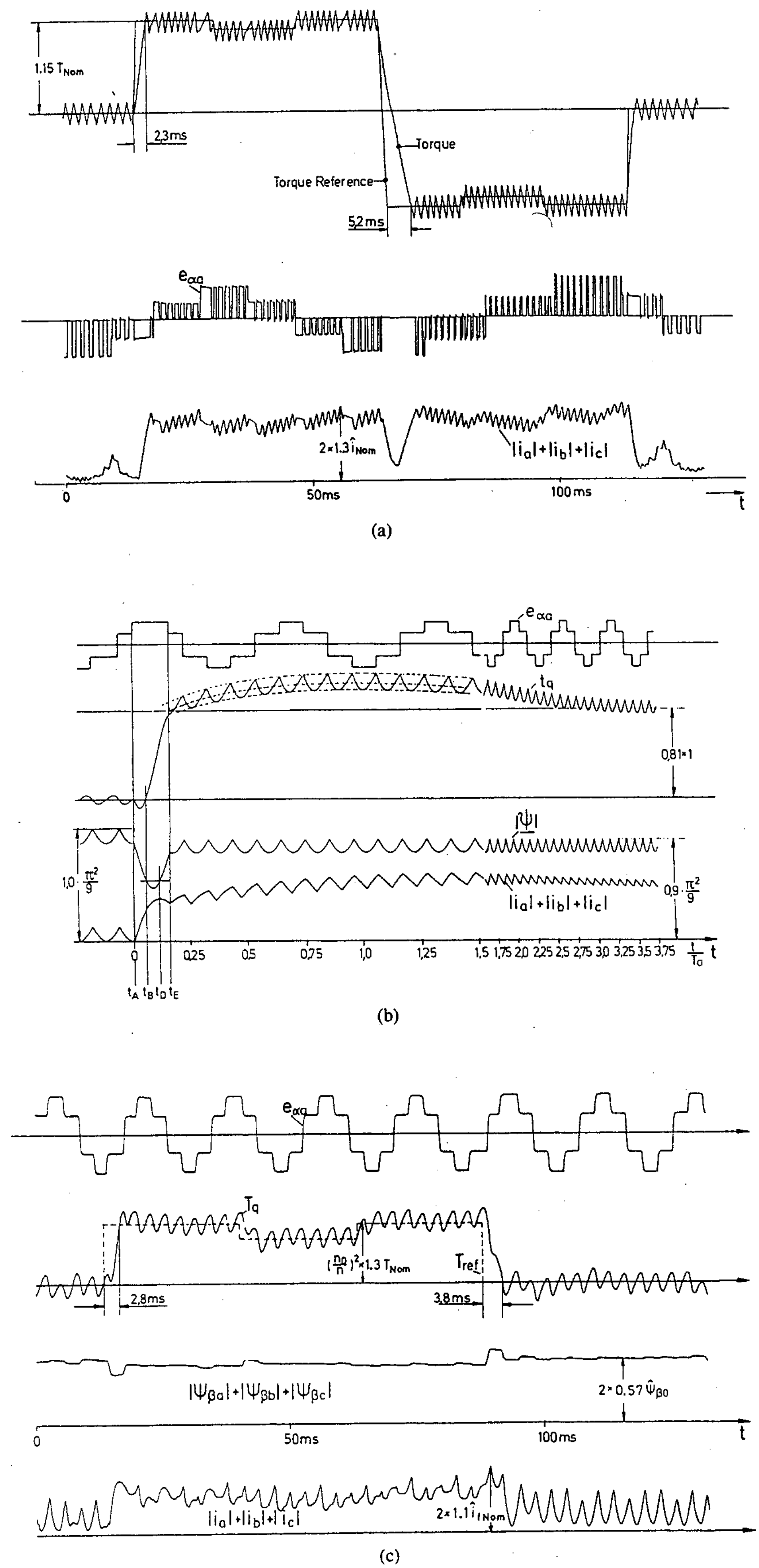

Fig. 9. Step response of induction machine with DSC.
(a) Experimental results: $\sigma = 8.5\%$, $T_\sigma = 52.5$ ms, $n_0 = 16.5$, $n/n_0 = 0.4$, $T_\sigma/T_\sigma'' \approx 1.5$ (T_σ'' ≙ subtransient value).
(b) Computer simulation: $n_0 = 9$, $n/n_0 = 1$, $t_q = T_q/T_{qK}$, $\psi = \Psi/\hat{\Psi}_{f\sigma}$.
(c) Experimental results: $\sigma = 6.1\%$, $T_\sigma = 33.6$ ms, $n_0 = 6.1$, $n/n_0 = 2$, $T_\sigma/T_\sigma'' \approx 1.5$ (T_σ'' ≙ subtransient value).

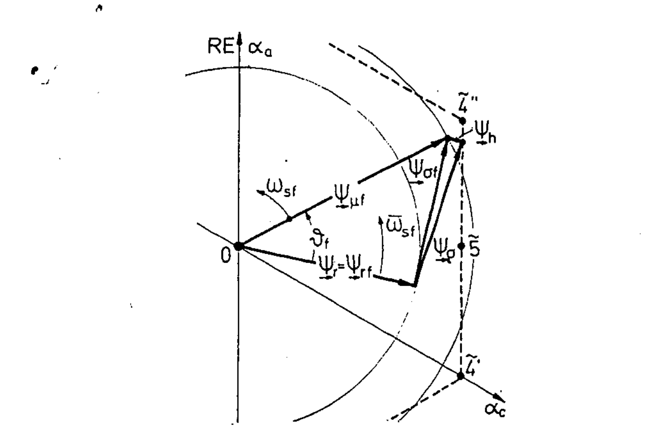

Fig. 10. Distorted track curve of total flux $\vec{\Psi}_\mu$ and fundamental track curves.

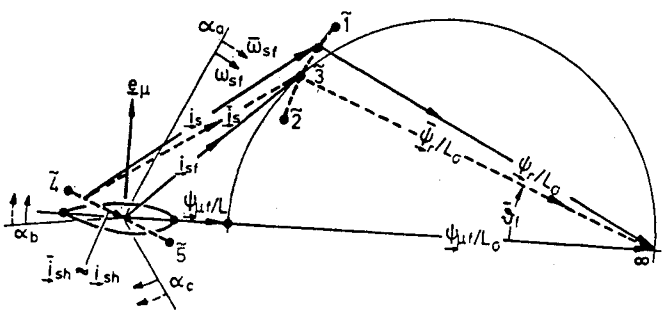

Fig. 11. Heyland diagram, completed by distortion quantities.

space vector of distortion portions of stator currents

$$\vec{i}_{sh} = \left(\frac{1}{L_\mu} + \frac{1}{L_\sigma}\right) \cdot \vec{\Psi}_h \tag{16}$$

to the tail of space vector $\vec{i}_{sf}$ in the origin of the diagram at each moment, the tail of space vector $\vec{i}_s$ of the resultant stator currents travels from point $\tilde{4}$ to point $\tilde{5}$ and back to $\tilde{4}$ six times within a period of stator quantities. In the limit case $T_p = 0$ the head of space vector $\vec{\bar{i}}_s$ is fixed to point $\tilde{3}$ on the Heyland circle; the track curve traversed by its tail in the limit case is a straight line which has the direction of space vector $\vec{\bar{\Psi}}_r/L_\sigma$ leading from point $\tilde{3}$ to point ∞ of the Heyland circle.

Compared to pure sinusoidal conditions, the harmonics of currents caused by a noncircular track curve of $\vec{\bar{\Psi}}_\mu$ increase only somewhat the RMS value of stator currents and normally their peak values, but at large values of torque ($\vartheta_f > 38.5°$) a hexagonal track curve leads even to peak values of stator currents slightly below the magnitude of their fundamentals. In reality the possible switching frequencies of VSI in heavy power applications are so low that distortion currents additional to those of the limit case at $T_p = 0$ and an alternating component of torque, all ringing at pulse frequency, cannot be neglected. If we now rotate the projection axes α_a, α_b, α_c with the instantaneous angular speeds zero or full nominal value ω_0, the space vector of rotor fluxes $\vec{\Psi}_r$ begins to move in the complex demonstration plane. Similar to the representation of Fig. 5, now the head of $\vec{i}_s$ travels from point $\tilde{1}$ to point $\tilde{2}$ and back to $\tilde{1}$ within each pulse period. If then the mean value of the speed, with which $\vec{\Psi}_\mu$ is running along the hexagonal track curve during each pulse period, agrees to that corresponding mean value of speed in the case of constant torque at $T_p = 0$, the tail of $\vec{i}_s$ furthermore approximately traverses the straight track curve between points $\tilde{4}$ and $\tilde{5}$ of Fig. 11. This happens in the case of two-point control of torque. If $\vec{\Psi}_\mu$ runs along its hexagonal track curve, keeping the mean value of track speed unchanged, now the tail of $\vec{i}_s$ in Fig. 11 traverses the droplet-shaped track curve around the origin of $\vec{i}_{sf}$ six times within a period of stator quantities. This happens, e.g., in the case of fundamental frequency switching. The droplet-shaped curve differs from the straight track curve of $\vec{\bar{i}}_{sh}$, because at a constant track speed of $\vec{\Psi}_\mu$ on its hexagonal track curve we cannot continuously give $\vec{\Psi}_h$ the direction of $\vec{\Psi}_r$. In the case of two-point torque control the magnitude of distortion currents and the alternating part of torque ringing at pulse frequency depends on the distance between points $\tilde{1}$ and $\tilde{2}$, which is proportional to pulse period T_p, if we keep all other parameters constant. At fixed mean value of VSI switching frequency, pulse periods get their lowest duration, if we keep the number of changes in the direction of track curve minimal. As can be seen from Fig. 2, a pulse period needs only two switchings if the direction of track curve is not changed and duration of the full voltage part of pulse period exceeds the allowed minimum time of VSI switching state, otherwise three switchings are needed per pulse period, which is an increase of 50 percent! To reduce the alternating portion of torque the hexagonal track curve of $\vec{\Psi}_\mu$ is optimal, because only six changes of its direction are needed. If the resultant distortion of stator currents is to be minimized below a limit value of the ratio between stator frequency and switching frequency, the next better approximation of the track curve to an ideal circle shape has to be chosen. Now the direction of the track curve is changed 18 times, which means we get a reduction of current distortion only at the cost of increased pulsation of torque compared to the case with a hexagonal shape of track curve. This shows that there is no simple rule to determine optimal shape of track curve; many conditions and parameters have to be considered, their relative importance depending strongly on the applications.

VII. Conclusions

Direct self-control is a method of simple signal processing which gives three-phase machines fed by VSI an excellent performance even at the low switching frequencies usual in heavy power applications. In the basic version of DSC the power semiconductors of a three-phase VSI are directly switched on and off via three Schmitt triggers, comparing the time integrals of line-to-line voltages to a reference value of desired flux, if the torque has not yet reached an upper limit value of a two-limit torque control. When the upper limit value is reached, zero voltages are switched on to the machine, as long as the lower limit value of torque is not yet underpassed. The track curve of a space vector of stator fluxes forms a hexagon. At a given switching frequency then the undesirable alternating component of torque becomes minimal. If at continuously switched-on full voltage the desired torque is not reached, field weakening is achieved by decreasing the reference value of flux. Dynamic properties of induction machines with DSC can be represented by response to step change of tracking speed of the flux space vector keeping the track curve constant and vice versa. If the well-known Heyland diagram is completed by simple transient locus lines, the results can be surveyed without difficulties at each point of duty. Computer simulations and experimental measurements confirm the validity of these theoretical investigations.

Acknowledgment

The author is grateful to Brown, Boveri & Co. AG, Mannheim, and Deutsche Forschungsgemeinschaft for supporting this investigation of DSC.

Nomenclature

a, b, c	Subscripts denoting names of phases.
ν	Subscript instead of a, b, or c.
$\alpha \cdots$	Subscripts for line-to-neutral phase quantities.
$\beta \cdots$ ab, bc, ac	Subscripts for line-to-line phase quantities.
μ, σ	*Subscript for magnetizing/leakage quantities.*
s, r	Subscript for stator/rotor quantities.
f	Subscript for fundamental components.
h	Subscript for harmonic distortion components.
K	Subscript for quantities at breakdown point.
0	Subscript for base values.
nom	Subscript for nominal values.
ref	Subscript for reference values.
$\rightarrow$	Arrow denoting space vectors, e.g., $\vec{e}_s$.
$\mathbf{a}$	Boldface denoting complex numbers, e.g., $\mathbf{a}$.
$\bar{\ }$	Overbar denoting mean values, e.g., $\bar{\omega}$.
$\sim$	Tilde denoting quantities at steady state.
$\wedge, \vee$	Caret/inverted caret denoting maximum/minimum values.
a	Control factor.
ϵ_T	Tolerance value of torque.
ϑ	Flux angle between $\vec{\Psi}_\mu$ and $\vec{\Psi}_r$.
ω^*	Angular speed of reference frame.
ω, n	Absolute/normalized angular frequency.
f	Frequency.
T_s	Period of stator quantities.
T_p	Pulse period.
T_σ	Rotor leakage time constant at low frequencies.
T''_σ	Rotor leakage time constant at high frequencies.
T_q, t_q	Absolute/normalized electromagnetic torque.
p_r, p_s	Complex eigenvalues.
L_μ, L_σ	Magnetizing/leakage inductance of equivalent circuit.
R_s, R'_r	Stator/rotor resistance of equivalent circuit.
σ	Leakage factor.
e	Voltage.
$2E_d$	Input dc voltage of inverter.
Ψ, ψ	Absolute/normalized flux.
i, y	Absolute/normalized current.

References

[1] F. Blaschke, "The method of field orientation for control of the rotating field machine," Dr. Thesis, Techn. Univ. Braunschweig, Germany 1984.

[2] S. Yamamura and S. Nakagawa, "Transient phenomena and control of ac servomotor—Proposal of field acceleration method," *Trans. B, IEE of Japan*, vol. 101-B, no. 9, pp. 557–563, Sept. 1981.

[3] J. Holtz and S. Stadtfeld, "A predictive controller for the stator current vector of ac-machines fed from a switched voltage source," *IPEC Tokyo Conf. Rec.*, pp. 1665–1675, 1983.

[4] T. Naguchi and I. Takahashi, "A new quick-response and high-efficiency control strategy of an induction motor," *IEEE Trans. Ind. Appl.*, vol. IA-22, pp. 820–827, Sept./Oct. 1986.

[5] M. Depenbrock (Inventor) "Direct self-control of the flux and rotary moment of a rotary-field machine," U.S. Patent 4,678,248.

[6] M. Depenbrock, "Direkte selbstregelung (DSR) für hochdynamische drehfeldantriebe mit stromrichterspeisung," *etz-Archiv*, Bd. 7, H.7, S.211–218, 1985.

[7] M. Depenbrock and T. Skrotzki, "Drehmomenteinstellung im feldschwächbereich bei stromrichtergespeisten drehfeldantrieben mit direkter selbstregelung (DSR)," *etz-Archiv*, Bd.9, H.1, S.3–8, 1987.

M. Depenbrock was born in Bielefeld, West Germany, on January 11, 1929. He studied electrical engineering at the Technical University of Hannover, receiving the Dipl.-Ing. degree in 1954 and the Dr.-Ing. degree in 1962.

From 1954 to 1962, while completing his studies, he worked in the Converter Research Laboratory of Brown, Boveri & Co. AG, Mannheim, West Germany. During 1962–1968 he continued his work at BBC Germany, first as Head of Central Staff for New Products and later as Head of Central Development of Electronic Hardware. In 1968 he became Professor of Electrical Engineering at Ruhr-University Bochum. His main research interests are in power electronics, ac drives, and the theory and measurement of reactive and apparent power.

Dr. Depenbrock received the VDI Honor Ring in 1969, an Award for Advanced Innovation in 1985, and the Heinrich Hertz Award in 1987. He is an Associate Editor of the journal *etz-Archiv*. Since 1962 he has been working in several national and international technical committees. He is an elected member of the Rheinisch-Westfalische Academy of Science.